

# Microfluidic add-on for standard electrophysiology chambers

Javeed Shaikh Mohammed,<sup>†a</sup> Hector Hugo Caicedo,<sup>†a</sup> Christopher P. Fall<sup>a,b</sup> and David T. Eddington<sup>\*a,c</sup>

Received 5th February 2008, Accepted 17th April 2008

First published as an Advance Article on the web 12th May 2008

DOI: 10.1039/b802037j

We have developed a microfluidic brain slice device ( $\mu$ BSD) that marries an off-the shelf brain slice perfusion chamber with an array of microfluidic channels set into the bottom surface of the chamber substrate. As this device is created through rapid prototyping, once optimized, it is trivial to replicate and share the devices with other investigators. The device integrates seamlessly into standard physiology and imaging chambers and it is immediately available to the whole slice physiology community. With this technology we can address the flow of neurochemicals and any other soluble factors to precise locations in the brain slice with the temporal profile we choose. Dopamine (DA) was chosen as a model neurotransmitter and we have quantified delivery in brain tissue using cyclic voltammetry (CV) and fluorescence imaging.

## Introduction

While the brain slice preparation has provided access to details of cellular and circuit level brain function, the relevance to the intact brain is always in question. There are two central problems with the current state of the art: obviously, and possibly unavoidably, the brain slice largely eliminates feed-forward and recurrent connections from distant brain areas, however specialized preparations are being developed to maintain these connections. But a second major problem is that it is very difficult to control the spatial and temporal neurochemical environment in a way that is relevant to the intact brain. Currently, virtually all brain slice physiology work is performed in some sort of variation on the open-well temperature controlled chamber with bath perfusion.<sup>1–4</sup> Improved methods to control the neurochemical microenvironment of the slice, while maintaining open access from the top for imaging and electrophysiology, are needed to better mimic the *in vivo* brain. This includes the transient application of experimental compounds, the maintenance of local gradients, and replication of differing microenvironments in different regions of the brain.

The current unmet experimental need for controlling the local neurochemical environment in the brain slice preparation provides the motivation for our development of the  $\mu$ BSD, however the device is broadly applicable to many tissue physiology problems. Bath perfusion allows us to alter the environment over the whole slice, and application of experimental compounds is possible using local pipette application, however, this is cumbersome when more than one pipette is used as there is a limited amount of space in the open bath perfusion and the apparatus can easily interfere with imaging and electro-

physiology assays due to the limited amount of space. Additionally, while there is a great deal of control for very small volumes, injecting large volumes into brain tissue may cause local tissue damage. Our design overcomes these issues by gently infusing compounds through the slice through a microfluidic substrate and eliminates the need for micromanipulators. By integrating a  $\mu$ BSD into a standard bath perfusion setup we are able to precisely control soluble factor delivery in space and time within a simple experimental setup that does not interfere with standard electrophysiology tools.

There have been several successful demonstrations of microfabrication applied to neurobiology,<sup>5</sup> however, to date there have been only two demonstrations of adapting these devices to *in vitro* preparations of cortical slices. One such example replaces the standard perfusion chamber with a custom microfluidic device employing laminar flow lines that sweep across the slice to expose different regions to different soluble signals.<sup>6</sup> Additionally, work in the Frazier lab has resulted in a microfabricated array of electrodes with embedded microfluidic channels for stimulation and recording within cortical slices.<sup>7</sup> Our approach aims to modify instead of replace standard experimental procedures to streamline experimental protocols and facilitate broad dissemination of our platform. In order for new technologies to be widely accepted they must not only provide a robust solution to a current experimental need, they must also be simple enough to seamlessly integrate into standard research labs. The  $\mu$ BSD satisfies both these requirements by allowing spatial and temporal control over neurotransmitter delivery with microscale precision (currently not possible), and this control is driven by replacing the glass bottom of a standard perfusion chamber with a membranous microfluidic network (simple) as illustrated in Fig. 1.

## Materials and methods

### Fabrication of the $\mu$ BSD

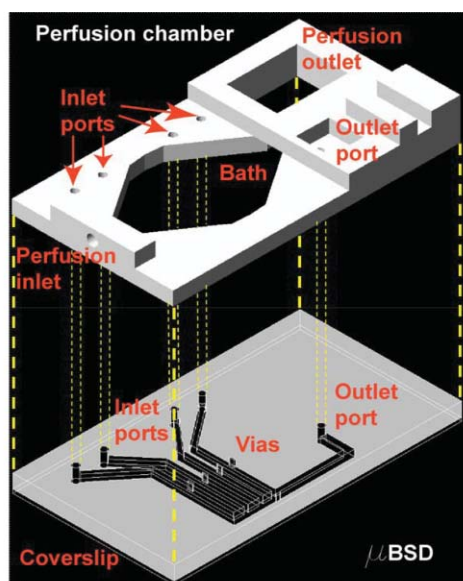
Standard rapid prototyping techniques<sup>8</sup> were used in the device fabrication. Details on this can be found elsewhere<sup>9</sup> and will be

<sup>a</sup>Department of Bioengineering, University of Illinois at Chicago, Chicago, IL, 60607–7052, USA

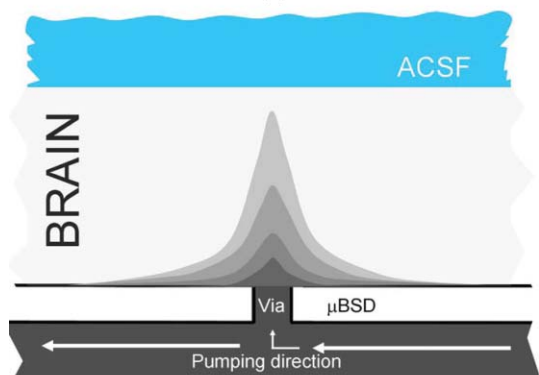
<sup>b</sup>Department of Anatomy & Cell Biology, University of Illinois at Chicago, Chicago, IL, 60607–7052, USA

<sup>c</sup>Department of Biopharmaceutical Sciences, University of Illinois at Chicago, Chicago, IL, 60607–7052, USA. E-mail: dte@uic.edu

<sup>†</sup> These authors contributed equally to this work.



(a)



(b)

**Fig. 1** Schematic representation of (a) how the  $\mu$ BSD docks to a standard perfusion chamber, (b) delivery of fluids into the cross-section of a brain slice. The ports on the  $\mu$ BSD are aligned with the ports on the standard perfusion chamber during the docking process. The perfusion chamber is filled with ACSF solution, and a brain slice is placed in the perfusion chamber bath above the vias. The solutions dispensed at the inlet ports are passively pumped through the microchannels and also driven into the brain slice through the vias.

briefly outlined below. The SU8 master was fabricated in a two step procedure as shown in Fig. 2. The two steps were used to fabricate a mold master with two heights, one for the microfluidic supply channels and one for vias, which refer to vertical openings or passages between layers.<sup>10</sup> The mask layout was designed in Adobe Illustrator 9.0 and printed onto a high resolution (5080 dpi) transparency film. The first SU8 layer was made to be 150  $\mu$ m (SU8-100 spun at 1800 rpm for 30 seconds). This layer consisted of the 250  $\mu$ m wide microfluidic supply channels (separated by 250  $\mu$ m), inlet and outlet ports, and alignment marks and was spun, softbaked, exposed, and post-exposure baked, but not developed. A second layer of SU8 was then spun onto the previously processed undeveloped layer to achieve 80  $\mu$ m (SU8-2050 spun at 1900 rpm for 30 seconds). The second layer consists of 75  $\mu$ m wide posts that are aligned onto the center of the first channels with the aid of alignment marks. Following

the second spin step the mold master was softbaked, exposed, post-exposure baked, and developed. Following development, the wafer was cleaned using isopropyl alcohol and finally dried in a stream of nitrogen gas.

Compression assisted micromolding techniques were then applied to fabricate the device using the two-layer mold master to achieve openings over the vias.<sup>11</sup> Prior to molding the polydimethylsiloxane (PDMS) (Sylgard 184), the alignment marks were removed with a razor as they were thicker than the microfluidic channels due to the edge bead effect. Support pillars made out of Scotch tape with thickness (130  $\mu$ m) less than the tallest structure on the wafer replace the alignment marks on four sides of the wafer to ensure the compression stack came in contact with the top of the via posts to achieve through holes. Four grams of a 10 : 1 mixture of PDMS (in a w/w ratio of base to curing agent), which had been degassed under vacuum, was poured onto the master. One end of a write-on transparency film was then placed on a hot plate and slowly placed on the PDMS solution so as to evenly spread the PDMS onto the master. If any bubbles were created during this process, they were manually removed. Four borofloat slabs (140 grams each) were placed on top of the wafer-transparency sandwich to apply constant pressure on the top surface of the cylindrical post structures during the curing process. Following removal of the PDMS membrane from the mold, after 2 h of curing at 75  $^{\circ}$ C, inlet and outlet ports were punched out with a blunted PS 15 Micro punch-hole 1.0 mm syringe needle. The membranous PDMS microfluidic network was then bonded to a 22  $\times$  40 mm coverglass substrate using oxygen plasma exposure at 165 Watts for 10 s (Terra Universal).

#### Docking the $\mu$ BSD substrate to a standard perfusion chamber

Four inlet and one outlet ports were drilled into the standard perfusion chamber (RC-26GPL, Warner Instruments) to ensure alignment of the ports (Fig. 1(a)) when the  $\mu$ BSD and the chamber were bonded together. Prior to docking the  $\mu$ BSD to the chamber, the bottom surface of the chamber was coated with PDMS to potentiate bonding between the chamber and the  $\mu$ BSD substrate.

#### Brain slice preparation

All procedures were approved by the Animal Care and Use Committee at the University of Illinois at Chicago. CD1 mice were anesthetized with AErrane (isoflurane, USP) and decerebrated. The frontal lobe was isolated in ice-cold standard solution and glued onto a tissue base. After slicing the tissue across the frontal lobe of the brain with a tissue slicer (VT1000S, Leica Microsystems Inc.) into 275–350  $\mu$ m thick sections, the brain slices were incubated in artificial cerebral spinal fluid (ACSF) standard solution (73.04 g NaCl, 21.84 g NaHCO<sub>3</sub>, 55.74 g glucose, 3.36 g NaH<sub>2</sub>PO<sub>4</sub> 7H<sub>2</sub>O, 1.87 g KCl, 1000 ml of DI water, 2.4 ml of CaCl<sub>2</sub> and 1.2 ml of MgCl<sub>2</sub>) which was continuously aspirated with 95% O<sub>2</sub>–5% CO<sub>2</sub> and maintained at 34  $^{\circ}$ C (for the initial 1 h and later at room temperature) before using them in experiments.

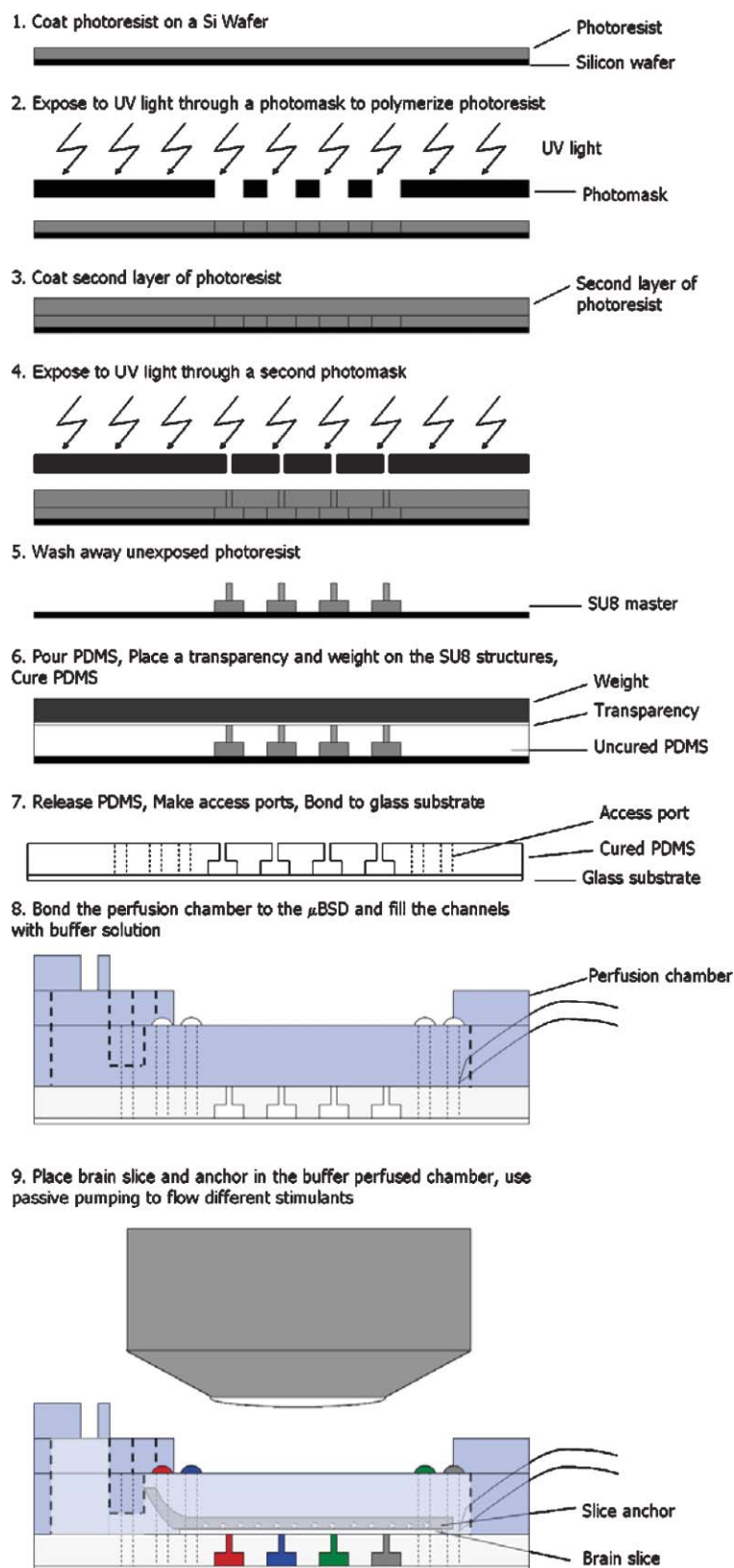


**Fig. 2** Schematic fabrication and integration flow-chart of the  $\mu$ BSD. Standard spinning, soft baking, UV exposure, and post exposure processes are used to fabricate the two-layer (150  $\mu$ m thick and 250  $\mu$ m wide microfluidic supply channels (separated by 250  $\mu$ m); 80  $\mu$ m thick and 75  $\mu$ m wide microposts) SU8 master and the  $\mu$ BSD. Standard rapid prototyping (compression assisted micromolding of PDMS) techniques are used to fabricate the  $\mu$ BSD using the two-layer mold master. The membranous PDMS microfluidic network is then bonded to a 22  $\times$  40 mm coverglass substrate using O<sub>2</sub> plasma exposure at 165 Watts for 10 s. Four inlet and one outlet ports were drilled into the standard perfusion chamber to ensure alignment of the ports (Fig. 1(a)) when the  $\mu$ BSD and the chamber (with PDMS coated bottom surface of the chamber) were bonded together.

## Device preparation and placement of tissue

The microchannels were filled with ACSF standard solution carefully to ensure minimal bubble introduction. Next, 80  $\mu\text{L}$  of ACSF solution were added to the outlet port to allow passive pumping of fluids from the inlet to the outlet ports of the  $\mu\text{BSD}$ . The  $\mu\text{BSD}$  was then immobilized in a plain platform (Model P-1, Warner Instruments), placed into the microscope adapter (SA-NIK, Warner Instruments), and integrated into a standard electrophysiology setup as shown in Fig. 3. The inlet and outlet tubing were connected to the perfusion chamber for continuous perfusion of the bath with ACSF solution (continuously aspirated with 95%  $\text{O}_2$ –5%  $\text{CO}_2$ ). Once the perfusion chamber was filled with ACSF solution, a brain slice was placed in the perfusion chamber bath. Using a probe, the brain slice was positioned over the circular vias in the microchannel network and then immobilized using a slice anchor (SHD-26GH/10, Warner Instruments).

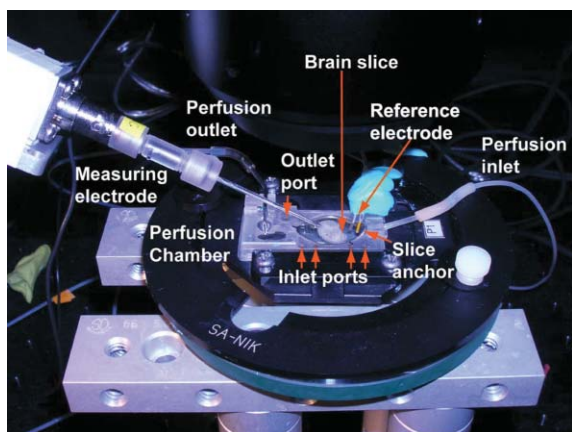


**Fig. 3** Image showing  $\mu\text{BSD}$  integrated with the electrophysiology setup. The  $\mu\text{BSD}$  is immobilized in a plain platform, placed into the microscope adapter, and integrated into a standard electrophysiology setup. The inlet and outlet tubing are connected to the perfusion chamber for continuous perfusion of the bath with ACSF solution (continuously aspirated with 95%  $\text{O}_2$ –5%  $\text{CO}_2$ ). The brain slice is placed in the ACSF filled perfusion chamber bath over the circular vias in the microchannel network and immobilized using a slice anchor. The levels of neurotransmitter delivered through the vias to the brain slice are measured amperometrically using the recording electrode.

## Fluid pumping method

Passive pumping<sup>12,13</sup> was employed to deliver the fluids through the microchannels as described previously. Briefly, 1  $\mu\text{L}$  of the fluid to be pumped through the channel was dispensed at the inlet port. As the radius of curvature of the drop at the inlet port was smaller than that of the drop (previously dispensed large drop of ACSF) at the outlet port, the fluid drop dispensed at the inlet port was pumped to the outlet port. Passive pumping was chosen to further streamline the setup by avoiding the need for tubing, connectors, and pumps which would interfere with an already complex electrophysiology setup. This method drives fluid through the via and into the tissue through both diffusion and convection. As the tissue has some inherent porosity,<sup>14</sup> the bolus is able to travel through the entire thickness of the tissue

and leach out due to convective flow of ACSF at the top of the slice preparation in the open bath.

## Validation of the fluid delivery scheme

**Without slice.** In order to validate the delivery scheme implemented through vias on top of the microchannels, a solution of fluorescein isothiocyanate (FITC) was used as a model soluble factor and the intensity was quantified with time-lapse fluorescence microscopy. FITC dye solution (1  $\mu\text{L}$  at 2  $\mu\text{M}$ ) dispensed at different inlet ports were passively pumped through the microchannels and also emerged into the perfusion chamber bath through vias. The FITC dye solution dispensing was chased by a bolus of ACSF to accurately quantify the amount of dye delivered through the via. These experiments were first done without a brain slice in the perfusion chamber to validate the microfluidic design, followed by similar experiments with a brain slice.

**With brain slice.** FITC dye solution was again used as a model soluble factor and the intensity was quantified with time-lapse fluorescence microscopy. FITC dye solution (1  $\mu\text{L}$  at 2  $\mu\text{M}$ ) dispensed at the inlet ports was passively pumped through the microchannels and also driven into the brain slice (Fig. 1(b)) through vias, and finally emerged into the perfusion chamber bath at the topside of the slice. Again, the FITC dye solution dispensing was immediately chased by a bolus of ACSF. MATLAB was used for image processing.

## Cyclic voltammetry measurements of DA delivery

Cyclic voltammetry is an electrochemical technique with high chemical selectivity and temporal resolution, and when used with a carbon fiber microelectrode it can be used to detect amperometric signature due to the oxidation and reduction of DA.<sup>15,16</sup> DA was used as a model neurotransmitter to quantify the delivery into the slice tissue. CV was used to amperometrically determine the DA levels delivered through vias of the  $\mu\text{BSD}$  to validate the delivery into the tissue.<sup>17–19</sup> The DA solution passed through the brain slice and exposed the tip of the recording electrode placed in the slice. The carbon fiber recording microelectrode was fabricated by threading a long carbon fiber into a glass micropipette followed by simultaneous dicing and sharpening of one end of the glass pipette using a Flaming/Brown type micropipette puller (P-97, Sutter Instrument Co.) to immobilize the fiber in the pipette. The carbon fiber tip was then cut to the desired length (100–300  $\mu\text{m}$ ) with a scalpel and the non-sharp end of the electrode threaded onto the conductive wire of a microelectrode holder (Dagan Corporation) and glued using conductive silver paint. The amperometric monitoring was performed using the fabricated recording electrode and an Ag/AgCl reference electrode and a custom cyclic voltammetry apparatus.<sup>17–19</sup> During these measurements, the brain slice was continuously perfused with ACSF standard solution aspirated with 95%  $\text{O}_2$ –5%  $\text{CO}_2$  and maintained at room temperature. Solutions (1  $\mu\text{L}$ ) of two different concentrations of DA (5 and 10 mM) were used in this experiment.

## Results and discussion

The current design of the  $\mu$ BSD consists of four parallel microchannels with individual inlet ports and a shared outlet port. As passive pumping is unidirectional towards the larger drop, we can have one outlet to simplify the device design without having any backflow. Each microchannel has a  $75\ \mu\text{m}$  circular via to connect the microfluidic channel to the perfusion bath. When the brain slice is positioned in the chamber and sealed to the bottom with the slice anchor, a fluidic seal is formed around the vias and different soluble factors can be delivered into the tissue through these vias. This overcomes the limitation with the existing microfluidic designs<sup>6,7</sup> where it is not possible to individually address different microscale areas of a brain slice region or different regions of a brain slice with soluble neurotransmitters. The number of vias and position are fixed for each device, but the device geometry can be easily changed depending on the needs of the experiment.

### Fluorescence imaging of compound delivery

In order to evaluate the functionality of the  $\mu$ BSD to deliver fluids through vias, FITC dye solution was used to monitor the time course of fluid delivery through the vias. Fig. 4(a) contains

a montage of fluorescence time-lapse micrographs obtained during the passive pumping of FITC ( $1\ \mu\text{L}$ ) through one of the microchannels of the  $\mu$ BSD. Here vias were not covered by a brain slice as this was meant to validate the microfluidic design; however, the bath contained ACSF solution. As evident from the images, the passive pumping method has been successfully applied to deliver FITC through the microfluidic channels and into the chamber. Immediately after the FITC solution was pumped through the channel, ACSF solution was pumped through that channel to wash out the FITC dye solution. This process of FITC pumping followed by the ACSF solution pumping through the channels was repeated in other channels to demonstrate rapid fluidic delivery in multiple adjacent regions. A similar approach was demonstrated previously for stimulating cultured neurons<sup>20</sup> and when a brain slice is placed onto the *via* the size of the exposed region will be much smaller as the dye flows much faster into ACSF than into the tissue. After validating the  $\mu$ BSD for fluid delivery without a brain slice, similar experiments were performed with a brain slice in the perfusion chamber.

The fluorescence micrograph in Fig. 4(b) shows a mouse brain slice placed on vias of the  $\mu$ BSD. The parallel threads of the slice anchor that hold the brain slice down onto the PDMS surface of the  $\mu$ BSD can be clearly seen running horizontally in the

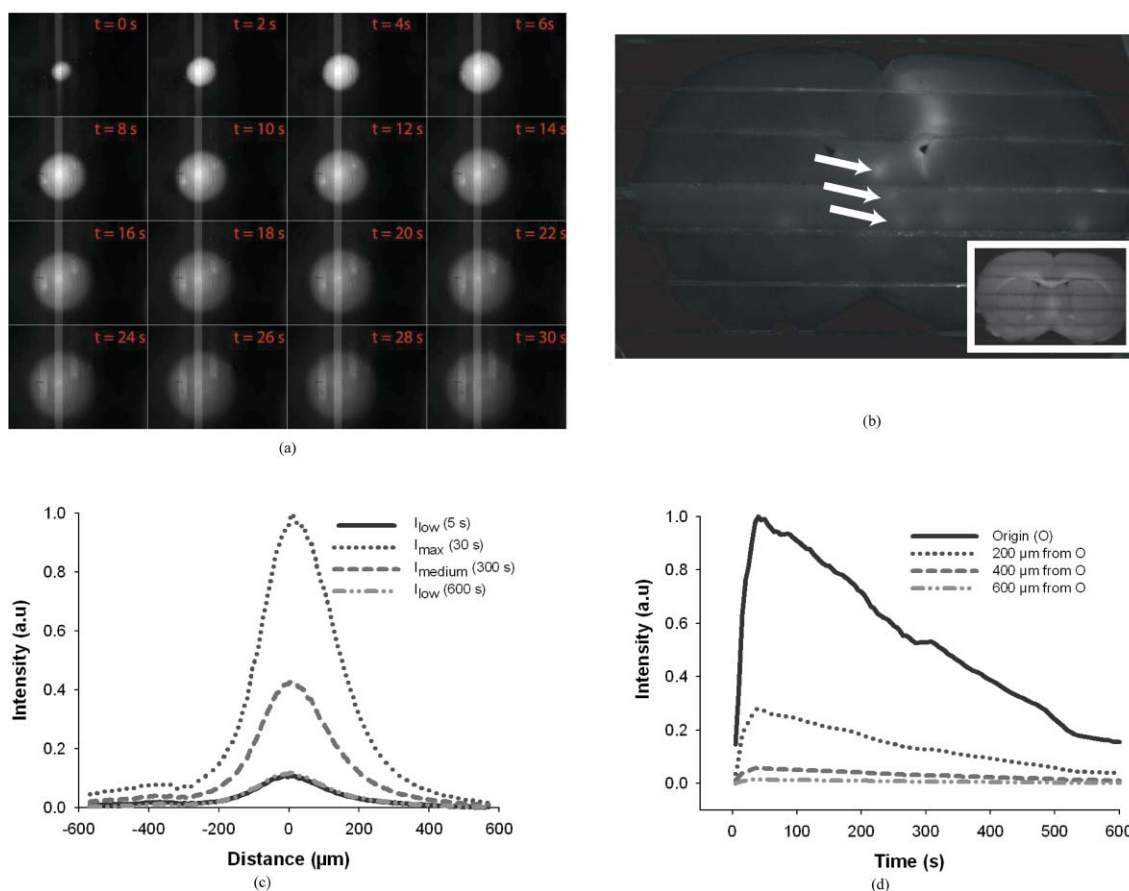


**Fig. 4** Without a brain slice: (a) Montage of fluorescence images (taken at 2 s intervals) showing FITC ( $1\ \mu\text{L}$  dispensed at the inlet port) in channels and delivered at a via. With a brain slice: (b) Fluorescence micrograph showing a mouse brain slice with FITC ( $1\ \mu\text{L}$  dispensed at the inlet port) spots as indicated by the arrows; the horizontal lines are threads of the slice anchor used to immobilize the brain slice. The inset is a bright field image of the same slice. (c) Spatial FITC fluorescence intensity profiles at  $t = 5, 30, 300,$  and  $600\ \text{s}$  after FITC dispersion at an inlet port. (d) Temporal FITC fluorescence intensity profiles at the center of a via [Origin (O)], at  $200, 400,$  and  $600\ \mu\text{m}$  distances from O.

micrograph. The arrows indicate the fluorescence spots in the brain slice created due to the FITC solution delivered through the vias in the PDMS surface present below these spots. This image illustrates the functionality of the  $\mu$ BSD to successfully deliver solutions in a controlled manner to microscale regions of the brain slice. The spacing and offset in the fluorescence spots corresponds to the spacing and offset of vias designed in the  $\mu$ BSD. The design can be altered to locate the vias in different regions of the brain slice, in different spatial arrangements within the same region of a brain slice, or with different spatial dimensions or shapes. To check that these spots were caused by dye diffusing into the tissue and not from an improper seal between the slice and the via, the slice was removed from the chamber and the spots remained in the tissue. Fig. 4(c) shows FITC fluorescence intensity at different times (5, 30, 300, and 600 seconds after FITC dispensation at an inlet port) along the diameter of a single *via* covered by a brain slice and at different distances from the center of the via. Fig. 4(d) shows FITC fluorescence intensity profiles as a function of time at different distances from the center of a via (0, 200, 400, and 600  $\mu$ m) after dispensing FITC dye solution at the inlet port. Again, the FITC dye solution traverses through the brain slice and finally into the ACSF solution in the bath as evident from the decreasing intensities and lack of broadening of the fluorescence intensity profiles. From the spatial FITC intensity profiles (Fig. 4(c)) 80% of the dye was within 400  $\mu$ m of the via, it can be estimated that the minimum separation between two adjacent vias should be 700  $\mu$ m to prevent overlap of fluids emerging from each via. From the spatial and temporal FITC intensity profiles (Fig. 4(c) and 4(d)) it is clear that the dye was driven into the brain slice and finally into the ACSF due to forced convection resulting from passive pumping through the porous structure of the slice. This is evident as if the transport was diffusion driven, the resulting fluorescence curve would be expected to broaden, the peak drop, and the baseline raise as time increased. Instead, the curve narrows while the peak drops and the baseline remains unchanged leading to the conclusion that the dye is flowing through and out of the slice. This is ideal for experiments requiring short term boluses of compounds as the injected compound can be easily flushed out by following with a bolus of ACSF. If longer stimulating time windows were needed, instead of a bolus of stimulant chased with ACSF, there could be multiple injections of the same compound. The fluorescence imaging data prove that the  $\mu$ BSD can successfully deliver soluble neurotransmitters to the bottom of brain slice tissues and the modulation of the brain slice tissue under different stimuli can be easily probed optically.

With our current design of the  $\mu$ BSD, the neurotransmitters can only be delivered at the bottom surface of the brain slices which is a limitation compared to the previously demonstrated designs.<sup>6,7</sup> Additionally, the passive pumping method for fluid delivery used here provides precise control over fluid delivery and eliminates the need for tubing, connectors, and pumps; however, it eliminates the advantage of automation in fluid delivery and increases the switching time between fluids delivered to the brain slices. It is important to note that we are currently limited to four separate inputs as we are relying on a standard perfusion chamber. However, future designs will alter the chamber area to allow more inputs or will use a separate manifold that connects

to the chamber to increase the number of distinct inputs. As there are only four vias in the current design, the placement of the slice is crucial to align the region of interest in the slice with the via to ensure proper delivery. However, future designs will increase the number of vias to allow easy access to many different regions of the slice. After validation of the fluid delivery scheme for the  $\mu$ BSD with fluorescence imaging experiments, we evaluated the delivery of DA using cyclic voltammetry to demonstrate standard electrophysiology apparatus is compatible with the  $\mu$ BSD.

### Cyclic voltammetry measurements of DA delivery into tissue

DA (1  $\mu$ L) was delivered through one of the vias to the brain slice and the levels of DA were measured amperometrically using a recording electrode as shown in Fig. 3. Initially, the relationship between the current measured using CV and the concentration of dopamine for the fabricated carbon fiber recording electrode was determined by positioning the electrode tip in close proximity to the orifice of a via (with no brain slice in the perfusion chamber) through which solutions of different concentrations of dopamine (0.625, 1.25, 2.5, 5, and 10 mM) were delivered as shown in Fig. 5(a). These measurements were made with the electrode placed above the via in the absence of a brain slice in the perfusion chamber. After establishing that the dopamine dose response relationship for that particular recording electrode was linear and the electrode was functional, the same electrode was used to measure the dopamine levels at the top surface of the slice. DA solutions (1  $\mu$ L) at two different concentrations (5 and 10 mM) were delivered to the brain slice as shown in Fig. 5(b). These plots demonstrate the current levels measured at a via with a brain slice are comparatively smaller than those measured without a brain slice. This indicates that the DA delivered at the bottom of the brain slice has passed through the brain slice and that the relative concentration at the top of the brain slice where the electrode was placed are lower compared at the bottom of the brain slice (that corresponds to the concentration of DA pumped). Nevertheless, in either case (with or without a brain slice) there is an increase in measured currents with increase in the DA concentrations. It is interesting to note the plot in Fig. 4(d) has a much sharper rise in intensity than Fig. 5(b). This is due to the fact that the fluorescence intensity was measured through the whole slice, thus averaging over the entire thickness, whereas the DA levels were measured near the surface of the slice closer to the ACSF in the chamber. Therefore, it takes longer for the DA to travel through the slice to the electrode at the opposite side than it takes for fluorescence to enter the slice. These results illustrate the overall functionality of the  $\mu$ BSD to successfully deliver solutions in a well controlled manner to selected regions of *in vitro* brain slices through a seamless integration of a  $\mu$ BSD substrate to a standard electrophysiology setup.

The  $\mu$ BSD is a simple and seamless addition to the standard electrophysiology setup that allows probing of brain slices for optical and electrical measurements. The  $\mu$ BSD is not a replacement of well-known methods for localized delivery of agents to slices *via* pipettes (pressure ejection or iontophoresis), but presents an alternative method for localized delivery of multiple agents. Pressure ejection through micropipettes remains the tool of choice when delivering a single factor to a single

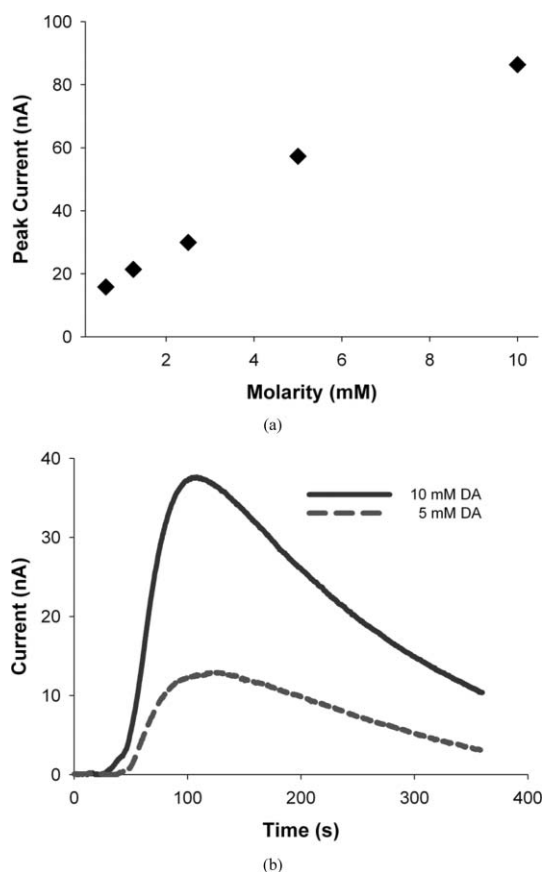


**Fig. 5** Without a brain slice: (a) DA dose response profile (relationship between the peak current measured using CV and the concentration of DA) for the recording electrode (positioned in close proximity to the orifice of a via) used in the CV measurements with a brain slice. With a brain slice: (b) Temporal current profiles measured at the slice–ACSF interface for DA solutions (1  $\mu$ L) at two different concentrations (5 and 10 mM) delivered to the brain slice.

region of a slice preparation as the dose can be very finely controlled. However, this method becomes too cumbersome when moving beyond one factor at one location as a separate micromanipulator and controller are required for each micropipette. Moreover, pipette application of compounds to the surface of the slice suffers from uncontrolled diffusion into the volume of perfusate, and pipette application of larger volumes into the tissue can result in disturbance of the tissue matrix. Pipette application therefore has limitations and drawbacks, and the  $\mu$ BSD provides complementary properties such as ease of multiple deliveries of multiple factors that is currently not possible or very difficult to achieve with current techniques. It is also important to note that the bolus delivery through passive pumping can be modulated through different sized openings and droplet volumes,<sup>13</sup> but will never reach the same level of control as with standard pipette delivery. However, this does not detract from the new possibilities available with the  $\mu$ BSD, including spatial patterns and standing gradients.

In future experiments we plan to extensively explore the spatiotemporal transport dynamics of neurotransmitters through different thicknesses of brain slices and in different regions of brain slice tissues using the  $\mu$ BSD. Delivery of compounds to different regions of a brain slice would require geometrical

modifications in the microchannel layout and would require multiple vias to deliver fluids to any specific region of the brain slice, but should not pose any unforeseen barriers. One example for an anticipated experimental use of the demonstrated  $\mu$ BSD is exploring how DA and other neuromodulatory agents might influence the ability of the prefrontal cortical microcircuit to maintain spatiotemporal activity patterns associated with working memory, cognitive flexibility and other executive functions.

## Conclusions

A simple and modular microfluidic add-on for standard perfusion chambers used in electrophysiology has been fabricated and demonstrated. The  $\mu$ BSD was integrated into a standard electrophysiology setup using an off-the-shelf perfusion chamber. Passive pumping was used to pump fluids through the channels. The fluorescence microscopy results indicate that fluids can be easily switched within a channel to control the amount of fluid delivered through a *via* and the fluid flow can be switched between different channels to allow delivery of fluids from different vias. The  $\mu$ BSD has been successfully applied to deliver fluids to specific regions of a brain slice. The CV measurements of DA levels measured with a brain slice in the perfusion chamber illustrate the feasibility of the  $\mu$ BSD for electrophysiological studies of brain slices. It is anticipated that the  $\mu$ BSD presented in this work will be widely applicable to different fields of tissue physiology.

## Acknowledgements

Funding was provided by NIH MH-64611 Career Award to CPF. The authors would like to thank Dr Mitchell Roitman for assistance with cyclic voltammetry. The authors would also like to acknowledge Adam Beagley, Mark Dikopf, Zenith Jameria, and Benjamin Smith for their technical assistance.

## References

- 1 P. A. Passeraub, A. C. Almeida and N. V. Thakor, *Biomed. Microdevices*, 2003, **5**, 147.
- 2 H. L. Haas, B. Schaerer and M. Vosmansky, *J. Neurosci. Methods*, 1979, **1**, 323.
- 3 R. Dingledine, J. Dodd and J. S. Kelly, *J. Neurosci. Methods*, 1980, **2**, 323–362.
- 4 S. R. Kelso, D. O. Nelson, N. L. Silva and J. A. Boulant, *Brain Res. Bull.*, 1983, **10**, 853–857.
- 5 D. B. Weibel, P. Garstecki and G. M. Whitesides, *Curr. Opin. Neurobiol.*, 2005, **15**, 560–567.
- 6 A. J. Blake, T. M. Pearce, N. S. Rao, S. M. Johnson and J. C. Williams, *Lab Chip*, 2007, **7**, 842–849.
- 7 Y. Choi, M. A. McClain, M. C. LaPlaca, A. B. Frazier and M. G. Allen, *Biomed. Microdevices*, 2007, **9**, 7–13.
- 8 Y. Xia and G. M. Whitesides, *Annu. Rev. Mater. Sci.*, 1998, **28**, 153–184.
- 9 J. Shaikh Mohammed, H. Caicedo, F. P. Christopher and T. D. Eddington, *J. Visual. Exp.*, 2007.
- 10 E. P. Kartalov, C. Walker, C. R. Taylor, W. F. Anderson and A. Scherer, *Proc. Natl. Acad. Sci. U. S. A.*, 2006, **103**, 12280–12284.
- 11 B.-H. Jo, L. M. Van Lerberghe, K. M. Motsegood and D. J. Beebe, *J. Microelectromech. Syst.*, 2000, **9**, 76.
- 12 G. M. Walker and D. J. Beebe, *Lab Chip*, 2002, **2**, 131.
- 13 E. Berthier and D. J. Beebe, *Lab Chip*, 2007, **7**, 1475–1478.
- 14 K. B. Neeves, C. T. Lo, C. P. Foley, W. M. Saltzman and W. L. Olbricht, *J. Controlled Release*, 2006, **111**, 252–262.

- 
- 15 D. L. Robinson, B. J. Venton, M. Heien and R. M. Wightman, *Clin. Chem. (Washington, D. C.)*, 2003, **49**, 1763–1773.
- 16 B. J. Venton and R. M. Wightman, *Anal. Chem.*, 2003, **75**, 414A–421A.
- 17 E. A. Budygin, M. R. Kilpatrick, R. R. Gainetdinov and R. M. Wightman, *Neurosci. Lett.*, 2000, **281**, 9–12.
- 18 D. J. Michael, J. D. Joseph, M. R. Kilpatrick, E. R. Travis and R. M. Wightman, *Anal. Chem.*, 1999, **71**, 3941–3947.
- 19 S. R. Jones, G. E. Mickelson, L. B. Collins, K. T. Kawagoe and R. M. Wightman, *J. Neurosci. Methods*, 1994, **52**, 1–10.
- 20 N. Mehenti, H. Fishman and S. Bent, *Biomed. Microdevices*, 2007, **9**, 579.